

Supporting information

Meis homeobox genes control progenitor competence in the retina.

Dupacova et al

SI Materials and Methods

Mice

Housing of mice and *in vivo* experiments were performed in compliance with the European Communities Council Directive of 24 November 1986 (86/609/EEC) and national and institutional guidelines. Animal care and experimental procedures were approved by the Animal Care Committee of the Institute of Molecular Genetics. A conditional mutant allele of the *Meis1* gene (*Meis1^{ff}*) was generated using *Meis1^{tm1a(EUCOMM)Hmgu}* embryonic stem cells (MGI ID: 4455660, Clone ID: HEPD0632_4_H07) purchased from EUCOMM. Mice carrying the *Meis1^{tm1a(EUCOMM)Hmgu}* allele were crossed with ACT-FLPe (stock no. 005703) to generate *Meis1^{ff}* mice by removing the promoter-driven cassette. These mice contain a conditional allele (*Meis1^{ff}*) wherein exon 8 of *Meis1^{ff}* is flanked by loxP sites. Cre-mediated recombination creates a frame shift mutation that results in a null allele. Sequence details for the *Meis1* targeting vector is available from EUCOMM (SI Appendix Fig. S13). *mRx-Cre* (1), *α-Cre* (2), *Meis2^{ff}* (3), *Pax6^{ff}* (4) and *ROSA26-EYFP* (5) mice have been described previously.

Tissue collections and histology

A minimum of three fields for a single eye and at least four offspring for each genotype at the same developmental stage were analysed and used for cell counting. Eye fields localized in a similar distance from the optic nerve were randomly selected.

Mouse embryos were harvested from timed pregnant females. The morning of vaginal plug was considered embryonic day (E) 0.5. For immunohistochemistry and haematoxylin-eosin staining, embryos and postnatal eyes were fixed by immersion in 4% paraformaldehyde overnight at 4°C. The samples were washed with ice-cold PBS, processed, embedded in paraffin, and sectioned (8µm). The paraffin sections were deparaffinised and then antigen retrieval was performed by boiling in sodium citrate buffer (10mM sodium citrate, 0.05% Tween 20, pH 6.0) for 20 minutes. The sections were permeabilized with PBT (PBS with 0.1% Tween 20), blocked with 10% BSA/PBT and incubated with primary antibody in 1% BSA/PBT overnight at 4°C. Slides were then washed in PBT and primary antibodies were detected by incubating with fluorescently-tagged secondary antibodies diluted 1:500 in 1% BSA/PBT for 30 minutes in the dark. Slides were washed in PBT and then nuclei were counterstained using DAPI. The images were taken with a Leica SP5 confocal microscope.

To detect *Meis1* and *Meis2*, sections were incubated in 0.3% H₂O₂ in methanol for 25 minutes after antigen retrieval. Slides were then washed with PBS, blocked with 10% BSA/PBT and

incubated with primary antibody in 1%BSA/PBT overnight at 4°C. The Vectastain ABC kit (Vector laboratories) was used for detecting primary antibodies. Antibodies used in this study were listed in *SI Appendix* table S1.

Measurement of cell cycle phase length

For analysis of all proliferation markers, a minimum of four animals from two individual litters were used. Wild-type littermates were used as control. Cell-cycle length was determined by sequential administration of two distinct thymidine analogues EdU and BrdU. First, timed pregnant females first received intraperitoneal injection of BrdU followed by EdU at 1.5 hours and were sacrificed at 2 hours. BrdU and EdU were detected using anti-BrdU antibody and the Click-iT EdU imaging Kit (Thermo Fisher Scientific), respectively. PCNA staining was used to identify proliferating retinal progenitor cells. The length of the cell cycle (T_c) and of S phase (T_s) in hours (h) was calculated as described previously (6, 7): $T_s = 1.5 \times S_{\text{cells}}/L_{\text{cells}}$ and $T_c = T_s \times P_{\text{cells}}/S_{\text{cells}}$ (L_{cells} : cells leaving S phase identified as BrdU⁺;EdU⁻, S_{cells} : cells in S-phase identified as EdU⁺ only and BrdU⁺;EdU⁺), P_{cells} : total proliferating cells identified as PCNA⁺ cells. All bar graph data were shown as mean \pm SEM. An unpaired two-tailed t-test was used to calculate statistical significance between samples. The p-values reported in each figure legend were labelled as follows: * $p < 0.05$, ** $p < 0.01$, and *** $p < 0.001$.

Bulk RNA-seq

Four biological replicates of *mRx-Cre* embryos and three biological replicates of *mRx-Cre;Mesi1^{ff};Meis1^{ff}* embryos were used for RNA-seq. *mRx-Cre;Mesi1^{ff};Meis2^{ff};ROSA26-EYFP* or *mRx-Cre;ROSA26-EYFP* retinæ at E14.5 were dissected in cold HBSS without Ca²⁺ and Mg²⁺. The isolated retinæ were incubated with 1 mg/ml dispase (Life Technologies) for 5 minutes at 37°C and then the supernatant was discarded. 1% FBS in HBSS without Ca²⁺ and Mg²⁺ was added and the samples were further dissociated by gentle trituration. Cells were then pelleted through centrifugation for 5 minutes at 300 X g. The supernatant was carefully aspirated off and resuspended with HBSS without Ca²⁺ and Mg²⁺. Cell aggregates were removed by straining cells through a 50 μ m filter. Cells were incubated with Hoechst 33342 (Molecular probes) and 50,000 X EYFP⁺;Hoechst⁻ cells were sorted into 500 μ l of RLT buffer using influx (BD Bioscience). RNA was isolated by Qiagen RNeasy Micro (Qiagen) according to the manufacturer's instructions.

RNA-seq libraries were prepared using NEBNext Ultra II Directional RNA Library Prep kit (NEB, E7760L) according to the manufacturer's instructions. Sequencing was performed with 75 bp single end sequencing by Illumina Nextseq 500 at the GeneCore facility of EMBL Heidelberg. RNA-seq reads were preprocessed with a FASTX tool kit v0.0.11 to remove short and low quality reads. RNA-seq reads were aligned to the mm10 genome using HISAT2 V2.1.0 (8). DESeq2 v1.1.25 (9) was used for differential gene expression analysis. A q-value cutoff of less than 0.05 was used for calling differentially expressed genes.

ChIP-seq

Timed-pregnant C57BL/6 mice were used for ChIP-seq. Three pools of samples were prepared and ChIP was performed three times. The retinæ at E14.5 were dissected, cross-linked with 1% formaldehyde at room temperature for 10 min, followed by quenching in 0.125M glycine for 5 min. The cross-linked retinal cells were lysed in 1% SDS lysis buffer (50mM Tris-HCl pH 8.0, 10mM EDTA, 1% SDS) containing proteinase inhibitors for 20 min on ice and sheared in a Bioruptor. Cell debris was removed by centrifugation. The supernatant was then diluted with ChIP dilution buffer ten times (16.7mM Tris-HCl pH 8.0, 1.2mM EDTA pH 8.0, 0.01% SDS, 1.1% Triton, 167mM NaCl) containing proteinase inhibitors. Thirty µg of sonicated chromatin was precleared with 30 µl of Dynabeads Protein G (Thermo Fisher Scientific) at 4°C for 3 hours. The precleared lysate was incubated either with anti-Meis1/2 (Santa Cruz biotechnologies) or anti-Meis1 (Abcam), or with rabbit IgG overnight at 4°C. Dynabeads Protein G was added and incubated for 3 hours. The beads containing the precipitated chromatin were then washed in low-salt washing buffer (20mM Tris-HCl pH 8.0, 2mM EDTA, 0.1% SDS, 1% Triton, 150mM NaCl), high-salt washing buffer (20mM Tris-HCl pH 8.0, 2mM EDTA, 0.1% SDS, 1% Triton, 500mM NaCl), LiCl washing buffer (10mM Tris-HCl pH 8.0, 1mM EDTA, 1% Na deoxycholate, 1% NP40, 250mM LiCl) and TE (10mM Tris-HCl pH 8.0, 1mM EDTA). The precipitated DNA was then eluted from the beads with ChIP elution buffer (10mM Tris-HCl pH 8.0, 1mM EDTA, 1% SDS) and de-crosslinked overnight at 65°C, followed by 1 hour of RNaseA treatment at 37°C and 2 hours of Proteinase K treatment at 55°C. The DNA was then purified with a MinElute PCR Purification kit (Qiagen) according to the manufacturer's instructions. ChIP-Seq libraries were prepared using an NEBNext Ultra II DNA Library Prep Kit (NEB, E7645L) and sequencing was performed with 50 bp single end sequencing by Illumina HiSeq 2000 at the GeneCore facility of EMBL Heidelberg.

ChIP-seq reads were pre-processed with FASTX tool kit v0.0.11. ChIP-seq reads were aligned to the mm10 genome by BWA aligner V0.7.17 (10). Peak calling was performed by HOMER V4.11 (11) using an FDR cutoff of 0.001, a cumulative Poisson p-value of <0.0001, and required a 4-fold enrichment of normalized sequenced reads in the Meis1 or Meis1/2 samples over the input sample. Density profiles of histone modification, ATAC-seq, and Lhx2 ChIP-seq around Meis1/2-bound sites were computed with ChAsE V1.1.2 (12). Overlaps between Meis1/2 and Lhx2 binding sites were determined using bedtools v2.29.2 (13). Meis1/2-bound genomic regions were tested with Homer V4.11 to detect enrichments of transcription factor binding motifs. In a 200 nucleotide sliding window of the mouse genome GRCm38 (GenBank accession number GCA_000001635.2), we checked the presence of the peak center and the presence of the Lhx2 motif TAATTA as published in the JASPAR database. Only windows without repetitive elements were used. Fisher's exact tests were done in R v4.0.2.

Lhx2 ChIP-seq (E14.5 retina) and Meis1 ChIP-seq (E10.5 whole eye) data were downloaded from GEO: GSE99818 and GSE62786, respectively (14, 15). ATAC-seq data (E14.5 retina) were downloaded from GEO: GSE87064 (16).

Generation of *Vsx2*Δ*CRM1*, *Vsx2*Δ*CRM2*, and *Vsx2*Δ*CRM1*&2 mice

Mice carrying deletions of *Vsx2* CRMs were generated using CRISPR-Cas9 technology. A complex of crRNA/TRACR (each at 10 μM, IDT) and SpCas9 protein (1.2 μM, IDT) was electroporated into fertilized zygotes isolated from *C57BL/6J* mice. Zygote electroporation and transfer into pseudopregnant foster females was performed as previously described (17). Founder animals from multiple embryo transfers were genotyped from tail biopsies using PCR and Sanger sequencing and the positive animals were backcrossed to *C57BL/6J* mice. Independent lines were established for *Vsx2*Δ*CRM1*, *Vsx2*Δ*CRM2*, and *Vsx2*Δ*CRM1*&2. Seven out of 22 carried either *CRM1* (3/22) or *CRM2* (5/22) and two out of 22 carried both *CRM1* and *CRM2* deletions (2/22). Since each of the founders displayed grossly similar homozygous phenotypes, one of them was chosen for further analysis. *Vsx2*Δ*CRM1* and *Vsx2*Δ*CRM2* contained 1452 bp deletion of *CRM1* and 978 bp deletion of *CRM2*, respectively. *Vsx2*Δ*CRM1*&2 contained 1452bp deletion of *CRM1* simultaneously with 1022 bp deletion of *CRM2*. At least four offspring for each genotype at the same developmental stage were analysed. The crRNAs targeting the following genomic sequences were used (PAM sequence underlined, *SI Appendix* Fig. S14):

*CRM1*_5' GATGGACTGCGGGTTGGACGGGG

CRM1_3' GAAATGGGTTGCAATCCTGGAGG

CRM2_5' TTTGAAGAGAGGCCGACTTGTTGG

CRM2_3' CGAAGCCGCTGAGTTGTGTGTTGG

The primers used for genotyping were listed in *SI Appendix* table S2.

The deletion junctions for the 3 lines are:

Vsx2ΔCRM1: 5'-AGGAAGATGGACTGC/AACCCATTTCCAACA-3'

Vsx2ΔCRM2: 5'-GAGCTGGGATTTAAC/TCAGCGGCTTCGCCT-3'

Vsx2ΔCRM1&2 at CRM1:

5'-TTGCAGGAAGATGGA/TTGCAACCCATTTCC-3'

Vsx2ΔCRM1&2 at CRM2

5'-AGCTGGGATTTAACC/TCTAGGCTCCTGACA-3'

Data availability

RNA-seq and ChIP-seq data have been deposited in the ArrayExpress database under accession numbers E-MTAB-9143 and E-MTAB-10112. Dataset S1 is available as part of the submission.

SI References

1. Klimova L, Lachova J, Machon O, Sedlacek R, & Kozmik Z (2013) Generation of mRx-Cre transgenic mouse line for efficient conditional gene deletion in early retinal progenitors. *PLoS One* 8(5):e63029.
2. Marquardt T, *et al.* (2001) Pax6 is required for the multipotent state of retinal progenitor cells. *Cell* 105(1):43-55.
3. Machon O, Masek J, Machonova O, Krauss S, & Kozmik Z (2015) Meis2 is essential for cranial and cardiac neural crest development. *BMC Dev Biol* 15:40.
4. Klimova L & Kozmik Z (2014) Stage-dependent requirement of neuroretinal Pax6 for lens and retina development. *Development* 141(6):1292-1302.
5. Srinivas S, *et al.* (2001) Cre reporter strains produced by targeted insertion of EYFP and ECFP into the ROSA26 locus. *BMC Dev Biol* 1:4.
6. Das G, Choi Y, Sicinski P, & Levine EM (2009) Cyclin D1 fine-tunes the neurogenic output of embryonic retinal progenitor cells. *Neural Dev* 4:15.

7. Martynoga B, Morrison H, Price DJ, & Mason JO (2005) Foxg1 is required for specification of ventral telencephalon and region-specific regulation of dorsal telencephalic precursor proliferation and apoptosis. *Dev Biol* 283(1):113-127.
8. Kim D, Paggi JM, Park C, Bennett C, & Salzberg SL (2019) Graph-based genome alignment and genotyping with HISAT2 and HISAT-genotype. *Nat Biotechnol* 37(8):907-+.
9. Love MI, Huber W, & Anders S (2014) Moderated estimation of fold change and dispersion for RNA-seq data with DESeq2. *Genome Biol* 15(12).
10. Li H & Durbin R (2009) Fast and accurate short read alignment with Burrows-Wheeler transform. *Bioinformatics* 25(14):1754-1760.
11. Heinz S, *et al.* (2010) Simple Combinations of Lineage-Determining Transcription Factors Prime cis-Regulatory Elements Required for Macrophage and B Cell Identities. *Mol Cell* 38(4):576-589.
12. Younesy H, *et al.* (2016) ChAsE: chromatin analysis and exploration tool. *Bioinformatics* 32(21):3324-3326.
13. Quinlan AR & Hall IM (2010) BEDTools: a flexible suite of utilities for comparing genomic features. *Bioinformatics* 26(6):841-842.
14. Marcos S, *et al.* (2015) Meis1 coordinates a network of genes implicated in eye development and microphthalmia. *Development* 142(17):3009-3020.
15. Zibetti C, Liu S, Wan J, Qian J, & Blackshaw S (2019) Epigenomic profiling of retinal progenitors reveals LHX2 is required for developmental regulation of open chromatin. *Commun Biol* 2:142.
16. Aldiri I, *et al.* (2017) The Dynamic Epigenetic Landscape of the Retina During Development, Reprogramming, and Tumorigenesis. *Neuron* 94(3):550-568 e510.
17. Jenickova I, *et al.* (2020) Efficient allele conversion in mouse zygotes and primary cells based on electroporation of Cre protein. *Methods*.

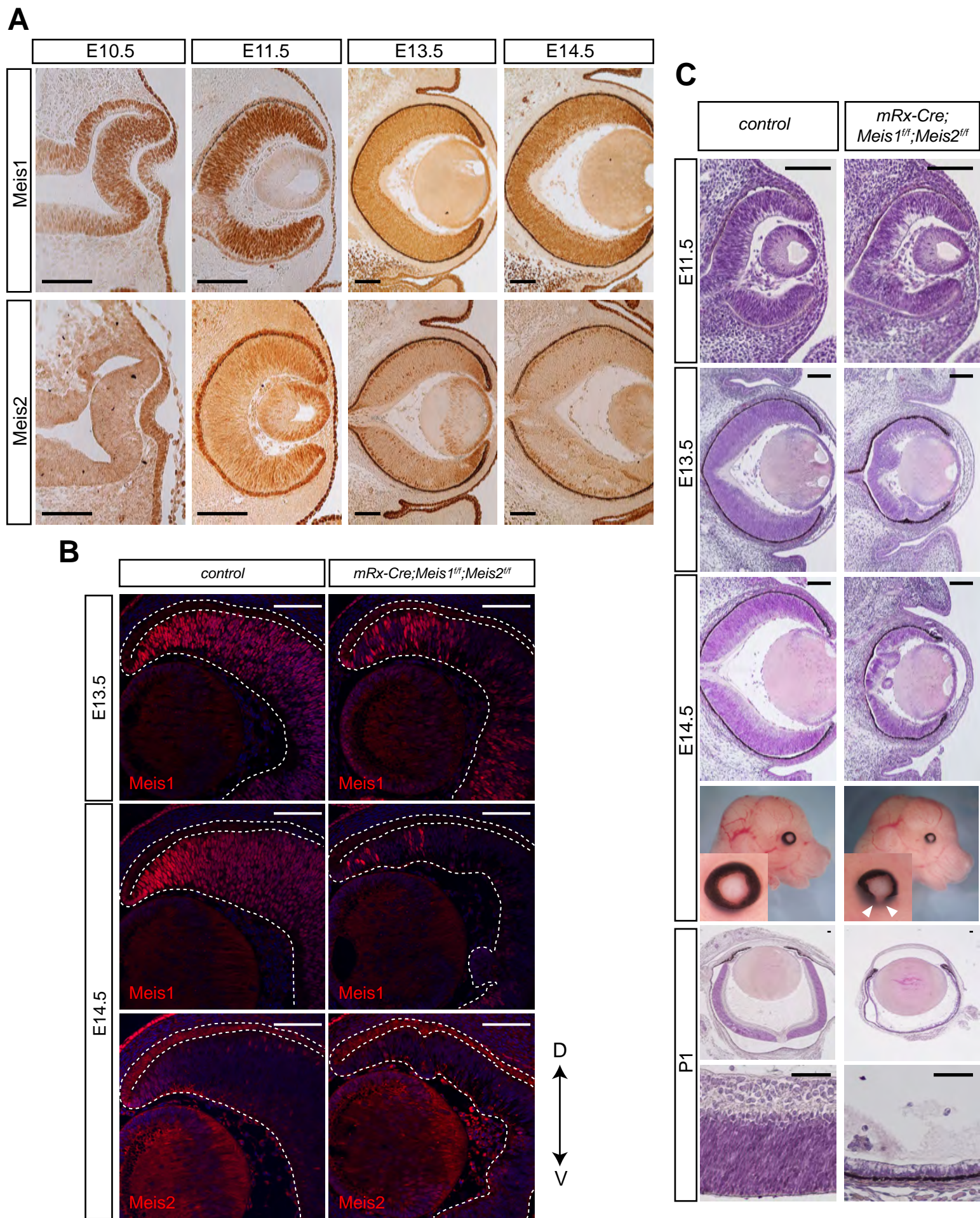


Fig. S1. Expression of *Meis1* and *Meis2* and phenotypic consequences of *Meis1/2*-deficient retina. (A) Immunostaining with *Meis1* and *Meis2* N-terminal antibodies in frontal sections of control and *Meis1/2* cKO embryos at indicated stages. (B) Immunostaining with *Meis1* and *Meis2* N-terminal antibodies in frontal sections of control and *Meis1/2* cKO embryos at E13.5 and E14.5. Melanin-bleaching was performed before immunostaining. (C) Haematoxylin-eosin-stained frontal sections and whole head of control and *Meis1/2* cKO embryos at indicated stages. Insets show high magnification views of the eyes. Arrow heads indicate coloboma. The dorsal-ventral axis is indicated by an arrow. D: dorsal, V: ventral, scale bars: 100 μ m

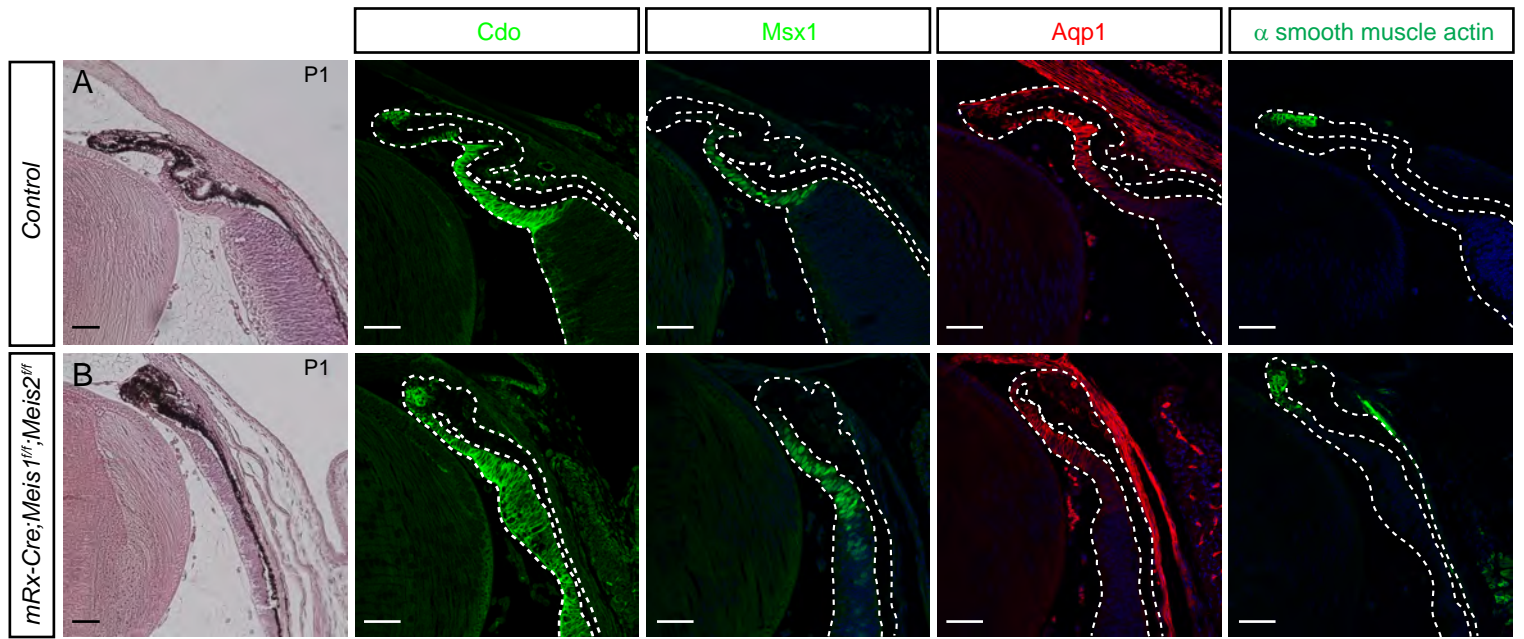


Fig. S2. Dysplasia of the iris and ciliary body in the *Meis1/2*-deficient retina. (A-B) Haematoxylin-eosin-stained retinal sections of control and *Meis1/2* cKO mice at P1. Immunostaining with Cdo, Msx1, Aqp1, and α -smooth muscle actin antibodies in retinal sections of control and *Meis1/2* cKO mice at P1. Scale bars: 50 μ m

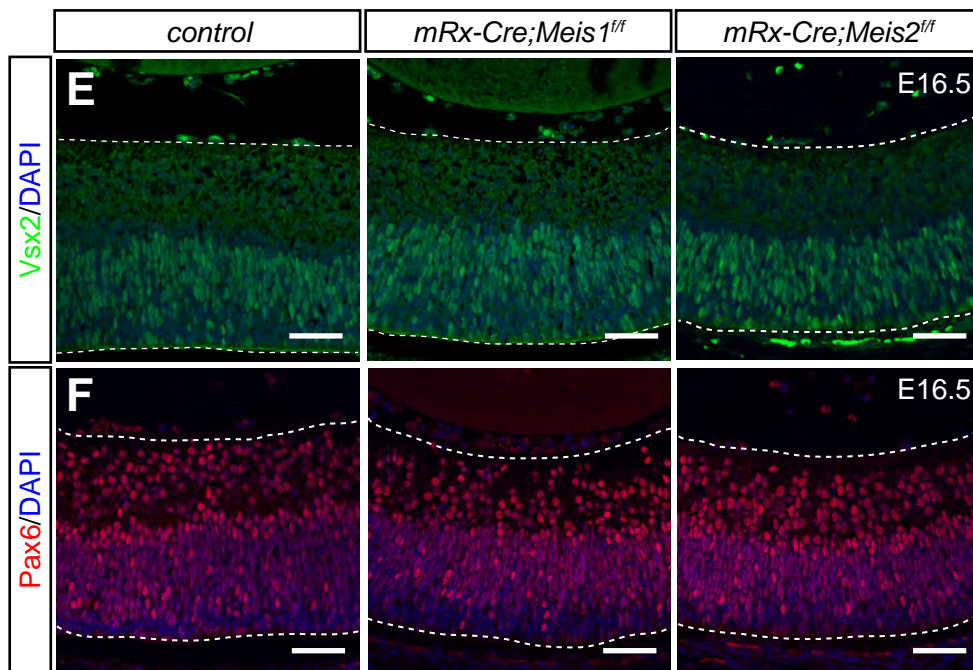
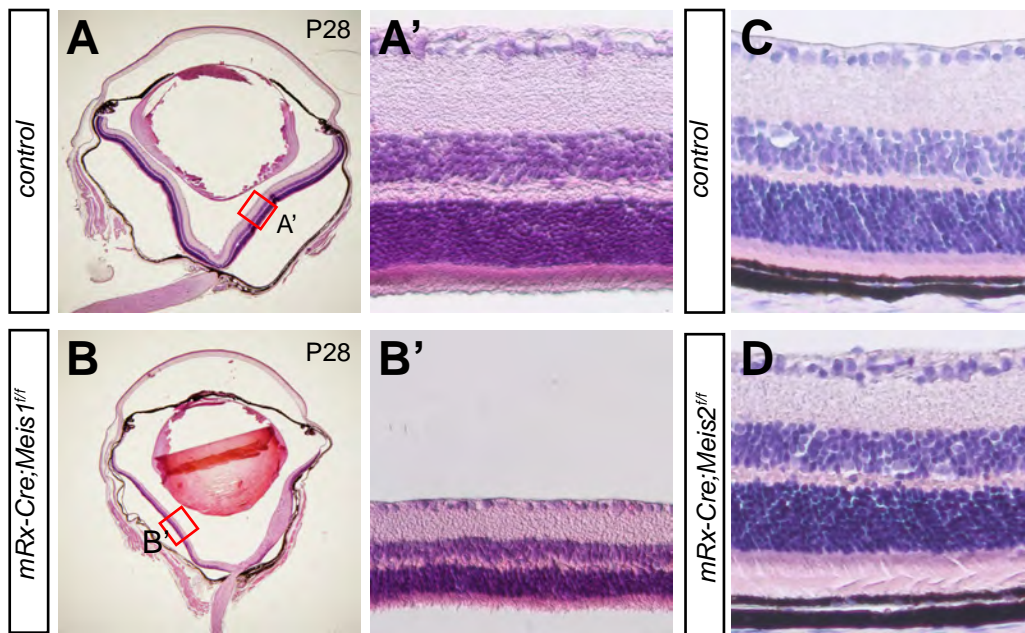


Fig. S3. Phenotypic consequence of *mRx-Cre;Meis1^{ff}* and *mRx-Cre;Meis2^{ff}* retinae. (A-D) Haematoxylin-eosin-stained paraffin sections of control, *mRx-Cre;Meis1^{ff}* and *mRx-Cre;Meis2^{ff}* at P28. (E-F) Immunostaining with Vsx2 and Pax6 antibodies in retinal sections of control, *mRx-Cre;Meis1^{ff}* and *mRx-Cre;Meis2^{ff}* at E16.5. Scale bars: 50 μ m

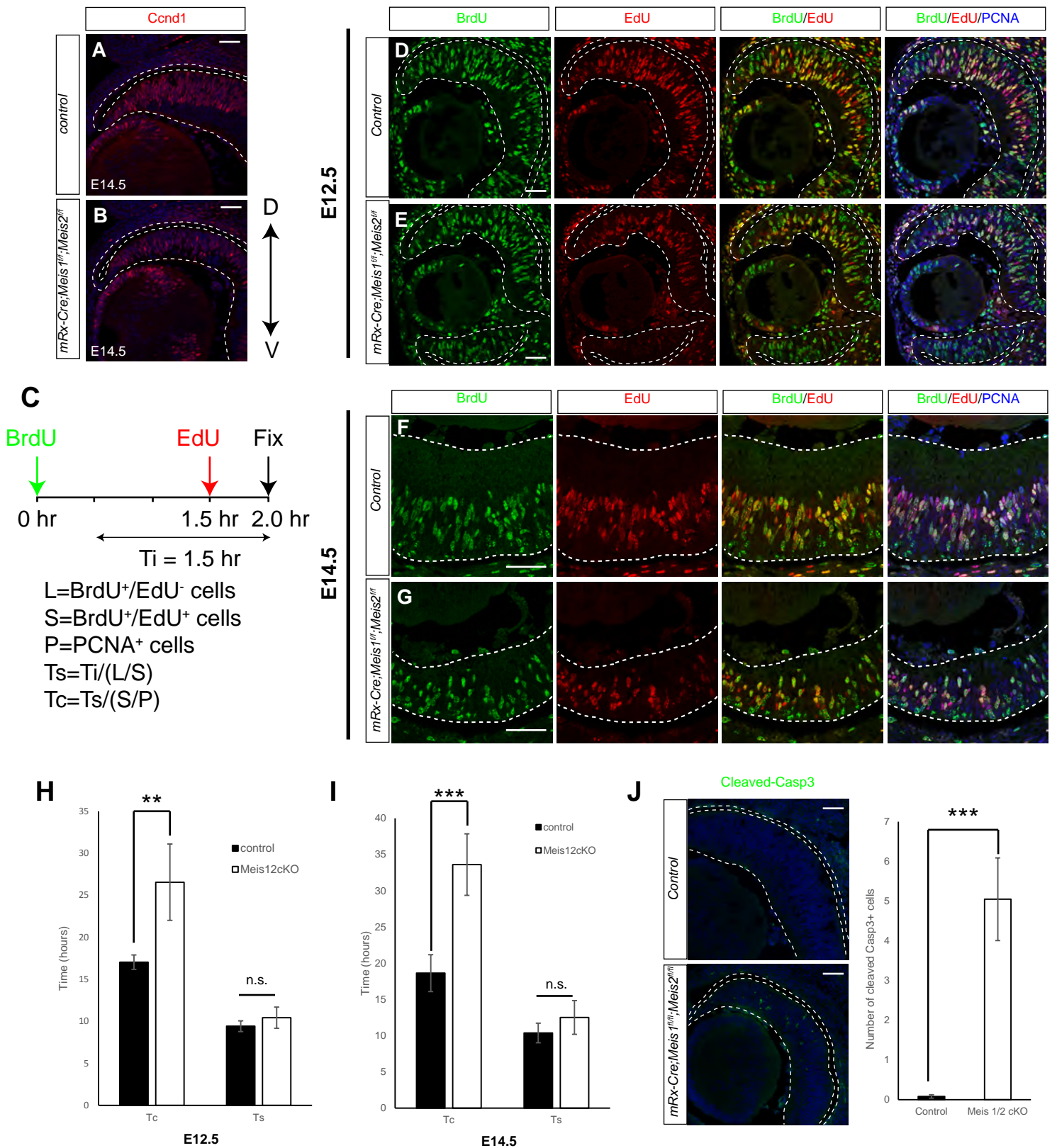


Fig. S4. Cell cycle of retinal progenitors is lengthened in the *Meis1/2*-deficient retina. (A-B) Immunostaining with *Ccnd1* antibody of frontal sections of control and *mRx-Cre;Meis1^{fl/fl};Meis2^{fl/fl}* embryos at E14.5. (C) Calculation of cell-cycle length. Sequential administration of BrdU and EdU estimates the total length of the cell cycle (Tc) and S-phase (Ts). (D-G) Immunostaining of frontal sections of control (D, F) and *mRx-Cre;Meis1^{fl/fl};Meis2^{fl/fl}* (E, G) embryos with BrdU, EdU, and PCNA antibodies at indicated stages. (H, I) Quantification of the total cell length (Tc) and S-phase (Ts) at indicated stages. (J) Immunostaining with cleaved caspase 3 antibody in frontal sections of control and *mRx-Cre;Meis1^{fl/fl};Meis2^{fl/fl}* embryos. Quantification of cleaved Caspase3⁺ cells. The dorsal-ventral axis is indicated by an arrow. D: Dorsal, V: Ventral. Scale bars: 50 μ m. ** $p < 0.01$, *** $p < 0.001$, $n = 6$

A

Gene	log2FC	FC	q-Value
Opn1sw	-6.65	-100.43	3.26E-03
Gnat2	-2.75	-6.73	8.14E-09
Lhx4	-2.55	-5.86	2.84E-08
Ptf1a	-1.53	-2.89	8.91E-06
Lgr5	-1.52	-2.87	9.62E-08
Tulp1	-1.46	-2.75	7.61E-04
Dlx2	-1.37	-2.58	6.32E-15
Barhl2	-1.34	-2.53	1.12E-11
Prdm1	-1.32	-2.5	6.63E-04
Tfap2a	-1.24	-2.36	1.42E-04
Eomes	-1.23	-2.35	9.06E-06
Prdm13	-1.22	-2.33	1.37E-12
Rorb	-1.18	-2.27	8.20E-37
Tfap2b	-1.13	-2.19	2.61E-13
Dlx1	-1.06	-2.08	4.77E-10
Otx2	-0.94	-1.92	2.71E-11
Tub	-0.92	-1.89	1.69E-16
Rxrg	-0.89	-1.85	2.55E-03
Tubb2a	-0.74	-1.66	1.07E-09
Pou4f2	-0.68	-1.6	7.98E-10
Thrb	-0.58	-1.49	2.68E-02

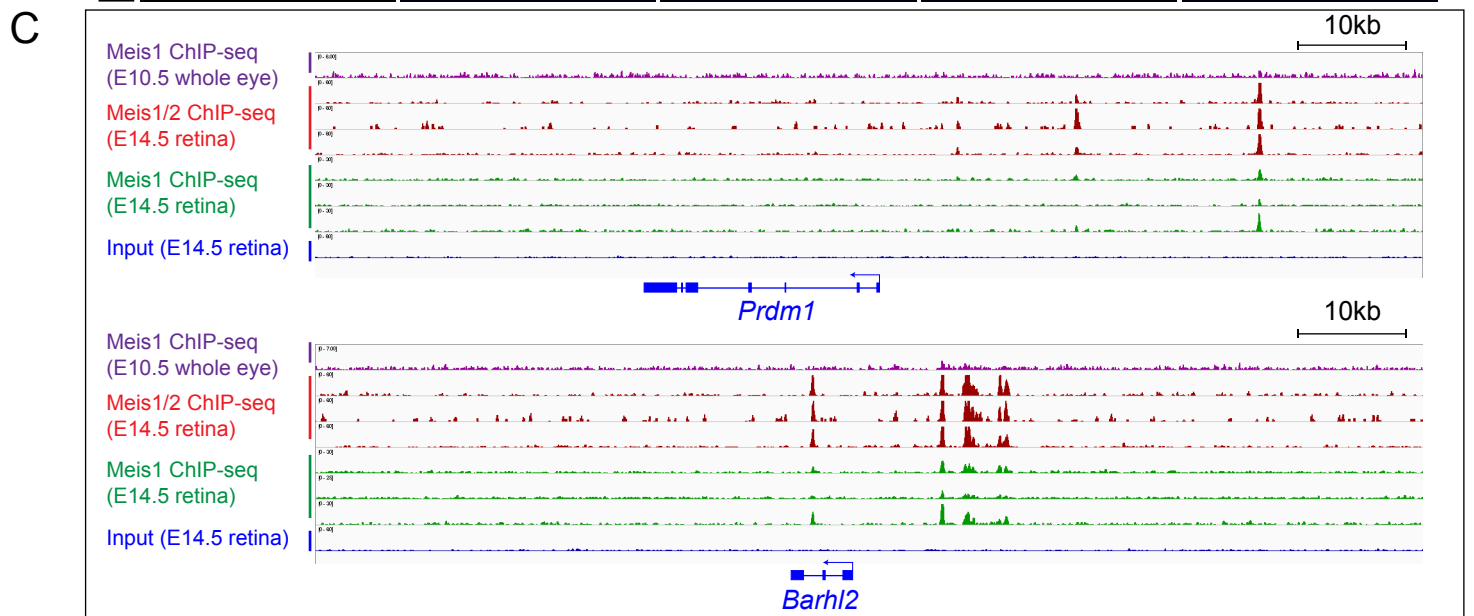
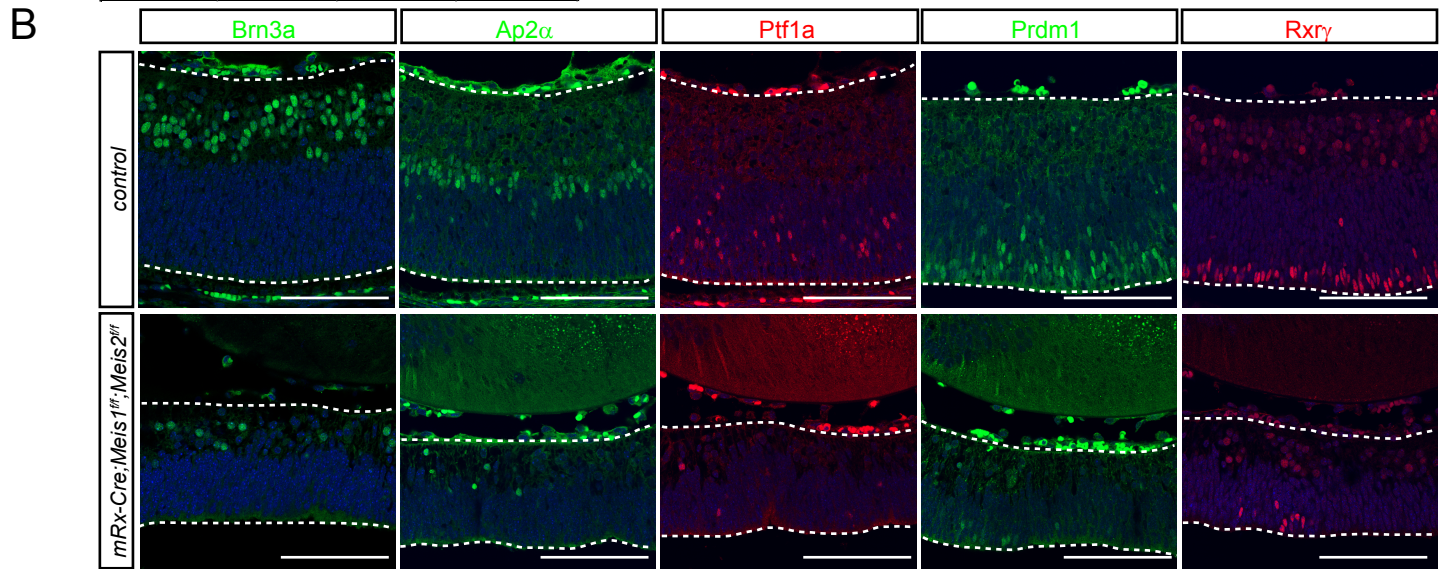


Fig. S5. Retinal ganglion (RGC), amacrine (AC), and cone photoreceptor (CP) specific genes are downregulated in the *Meis1/2* cKO retina. (A) A list of downregulated genes characteristic of RGC, AM, and CP in the *Meis1/2* cKO retina at E14.5. (B) Immunostaining with Brn3a, Ap2a, Ptf1a, Prdm1, and Rxrg antibodies in retinal sections of control and *Meis1/2* cKO embryos at E16.5. (C) ChIP-seq showing Meis1/2 or Meis1 binding at the *Prdm1* and *Barhl2* loci. (E14.5 retina Meis1/2 and Meis1 ChIP-seq: E-MTAB-10112 (this study), E10.5 whole eye Meis1 ChIP-seq: GSE62786 (14)). Scale bar: 100 μ m.

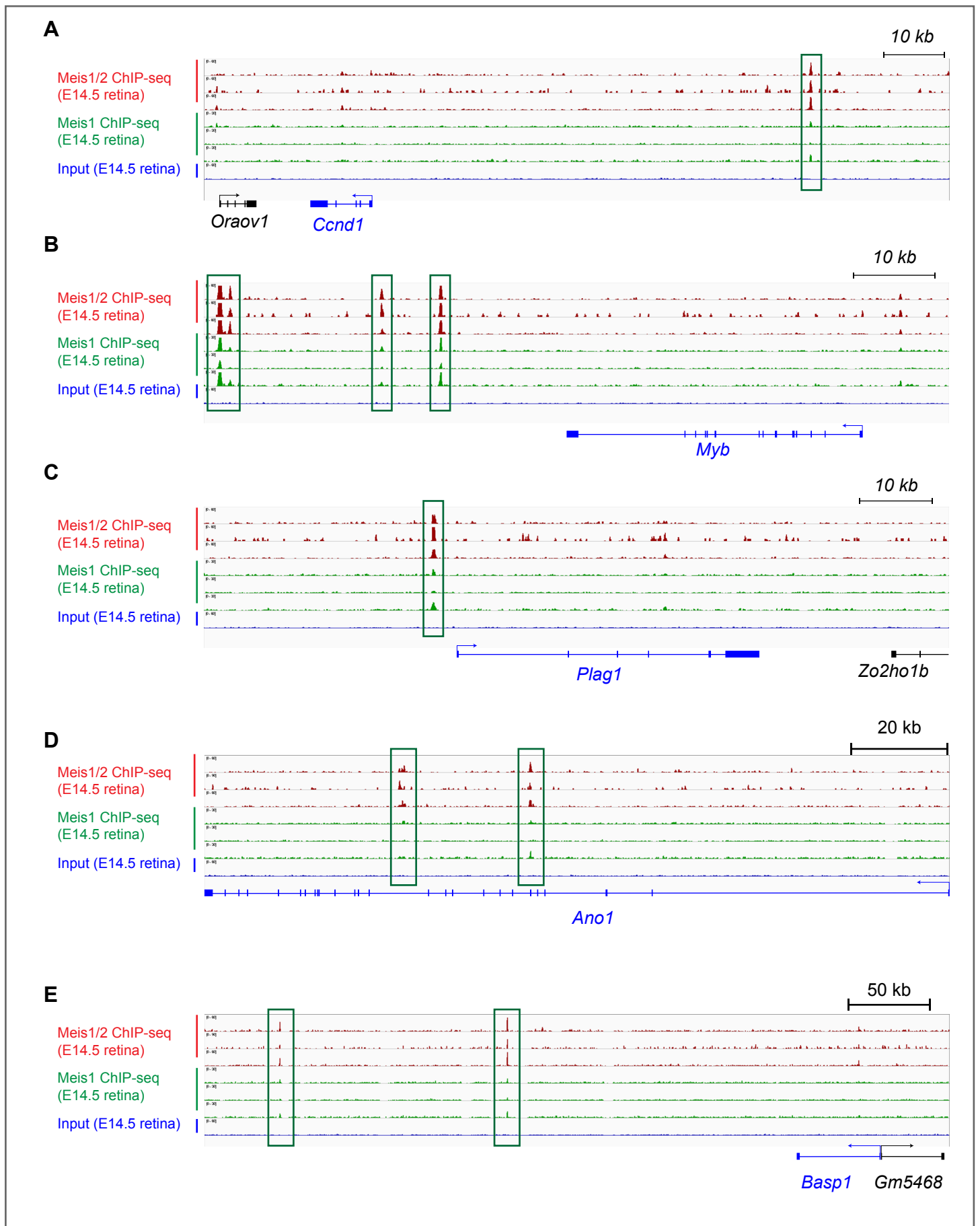


Fig. S6. Meis1 and 2 bind to cell cycle-related gene enhancers. (A-E) ChIP-seq showing Meis1/2 or Meis1 binding at *Ccnd1* (A), *Myb* (B), *Plag1* (C), *Ano1* (D), and *Basp1* (E) loci. E14.5 retina Meis1/2 and Meis1 ChIP-seq: E-MTAB-10112 (this study).

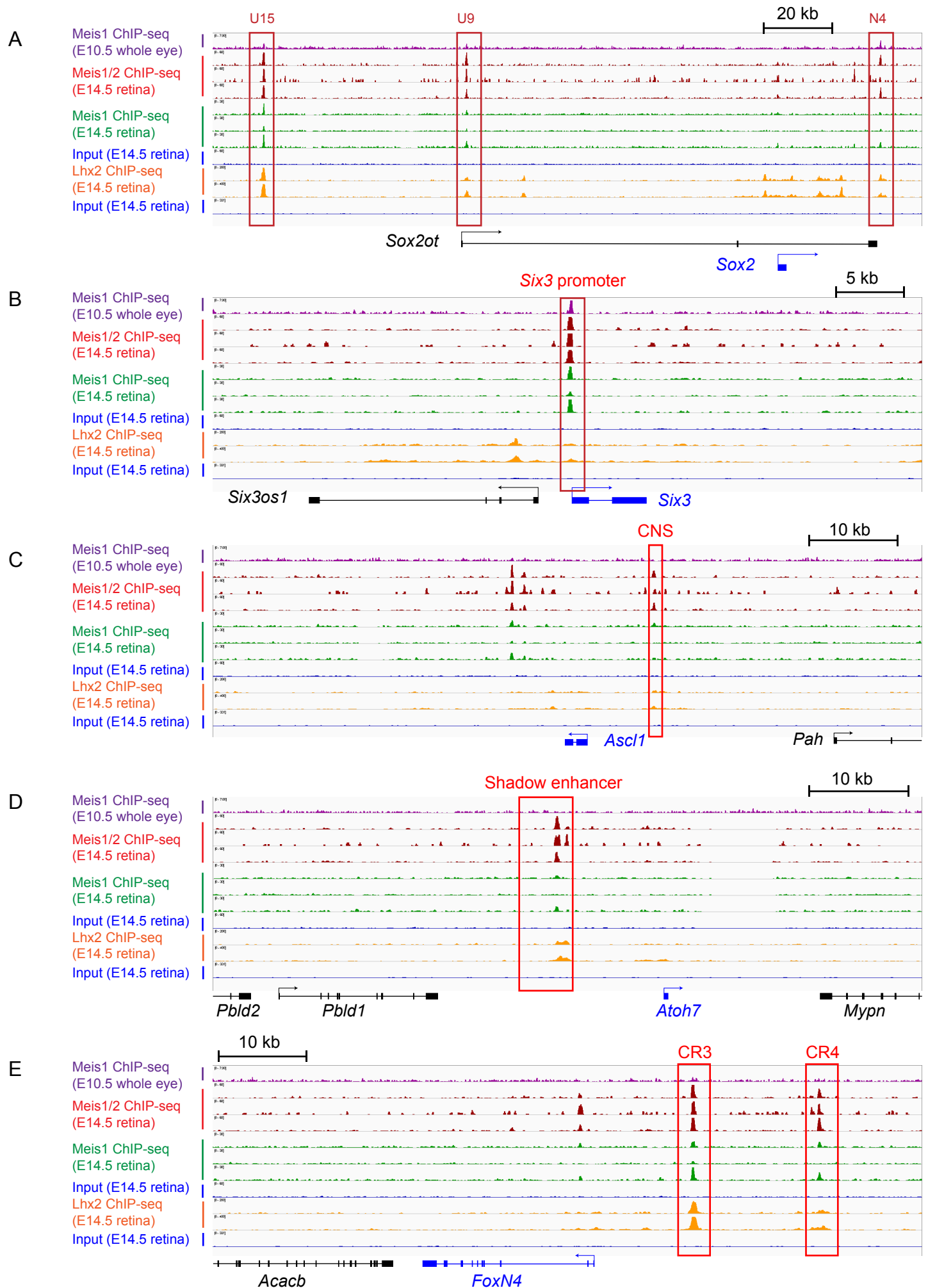


Fig. S7. Meis binding sites in the neuroepithelium at E10.5, in RPC at E14.5 and Lhx2 binding sites in RPC at E14.5. (A-F) E14.5 retina Meis1/2 ChIP-seq (E-MTAB-10112, this study), E10.5 whole eye Meis1 ChIP-seq (GSE62786, (14)), and E14.5 retina Lhx2 ChIP-seq (GSE99818, (15)) showing Meis1/2 or Meis1 binding at *Sox2* (A), *Six3* (B), *Ascl1* (C), *Atoh7* (D), and *FoxN4* (E) loci.

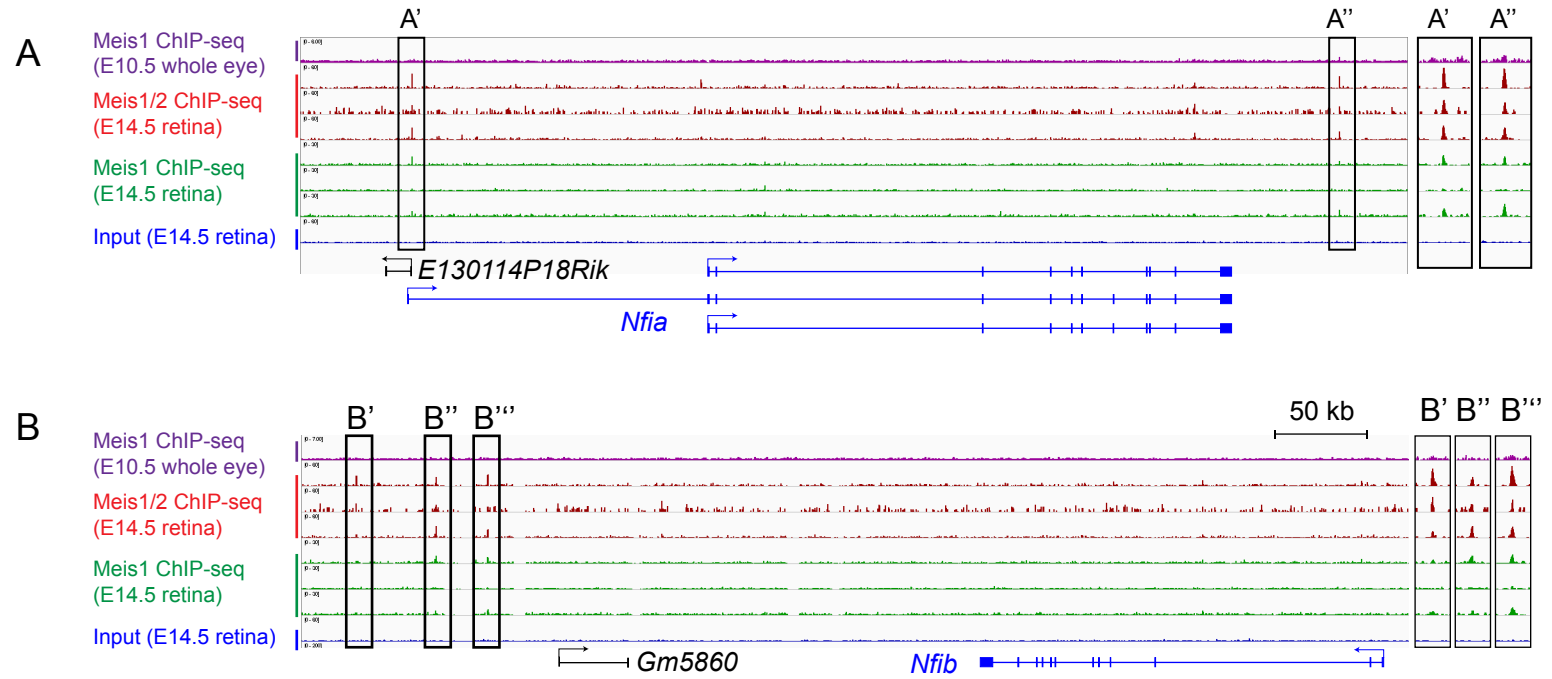


Fig. S8. Meis binding sites in the neuroepithelium and in RPC. E14.5 retina Meis1/2 ChIP-seq and E10.5 whole eye Meis1 ChIP-seq showing Meis1/2 or Meis1 binding at *Nfia* (A) and *Nfib* (B). Magnified view of boxed areas in A and B, which are noted as A', A'', B', B'' and B''', are shown in right panels. E14.5 retina Meis1/2 ChIP-seq: E-MTAB-10112, this study, E10.5 whole eye Meis1 ChIP-seq: GSE62786 (14).

A

	log2FC	fold change	q-value
Msx2	8.75E+00	430.54	7.05E-07
Tfec	7.07E+00	134.36	1.83E-03
Slc38a5	5.58E+00	47.84	2.63E-03
Irs4	4.50E+00	22.63	1.93E-40
Bmp4	4.29E+00	19.56	9.17E-22
Otx1	3.11E+00	8.63	4.15E-07
Mitf	2.73E+00	6.63	2.15E-05
Lrp2	2.49E+00	5.62	1.07E-20
Igf2	2.48E+00	5.58	6.26E-18
Npnt	2.34E+00	5.06	1.36E-06
Foxp2	2.28E+00	4.86	2.72E-22
H19	2.00E+00	4.00	2.60E-54
Rlbp1	1.98E+00	3.94	6.07E-04
Col18a1	1.61E+00	3.05	8.05E-47
Zic1	1.46E+00	2.75	8.60E-41
Ccnd2	1.40E+00	2.64	4.69E-10
Tgfb2	1.30E+00	2.46	2.09E-24
Sgk1	1.30E+00	2.46	6.94E-03
Crhbp	1.22E+00	2.33	1.09E-08
Ccne1	1.07E+00	2.10	3.55E-05
Myc	9.80E-01	1.97	6.96E-06
Fzd4	9.06E-01	1.87	1.20E-02
Fgfr2	8.80E-01	1.84	4.39E-02
Vcl	8.43E-01	1.79	4.21E-02
Bmp7	8.37E-01	1.79	1.93E-02
Notch2	7.94E-01	1.73	2.00E-04
Ltbp1	7.31E-01	1.66	5.96E-02
Gas1	7.15E-01	1.64	4.10E-03
Cst3	7.14E-01	1.64	5.18E-09
Cdo	6.53E-01	1.57	7.86E-08
Yap1	6.18E-01	1.53	8.37E-07
Nr2f1	5.96E-01	1.51	1.21E-08

B

	log2 FC	fold change	q-value
Fzd1	3.53E+00	11.55	2.64E-111
Fzd8	2.14E+00	4.41	1.73E-25
Wnt7b	1.94E+00	3.84	2.68E-10
Fzd7	1.50E+00	2.83	7.40E-16
Wnt5b	1.38E+00	2.6	1.41E-07
Wnt5a	1.28E+00	2.43	7.10E-04
Tcf7	1.27E+00	2.41	1.80E-04
Tcf7l2	1.09E+00	2.13	1.52E-17
Fzd5	9.78E-01	1.97	3.80E-27
Tcf7l1	9.26E-01	1.9	1.20E-05
Fzd4	9.06E-01	1.87	1.20E-02
Fzd3	7.19E-01	1.65	1.32E-10

C

	log2 FC	fold change	q-value
Bmp2	5.37E+00	41.36	2.32E-02
Bmp4	4.29E+00	19.56	9.17E-22
Bmper	1.78E+00	3.43	1.52E-02
Bmpr1b	1.73E+00	3.32	6.30E-42
Bmp1	8.64E-01	1.82	1.25E-08
Bmp7	8.37E-01	1.79	1.93E-02

Fig. S10. Lists of upregulated genes characteristic of CMZ (A), Wnt signalling (B) and Bmp signaling (C) in the *Meis1/2* cKO retina at E14.5.

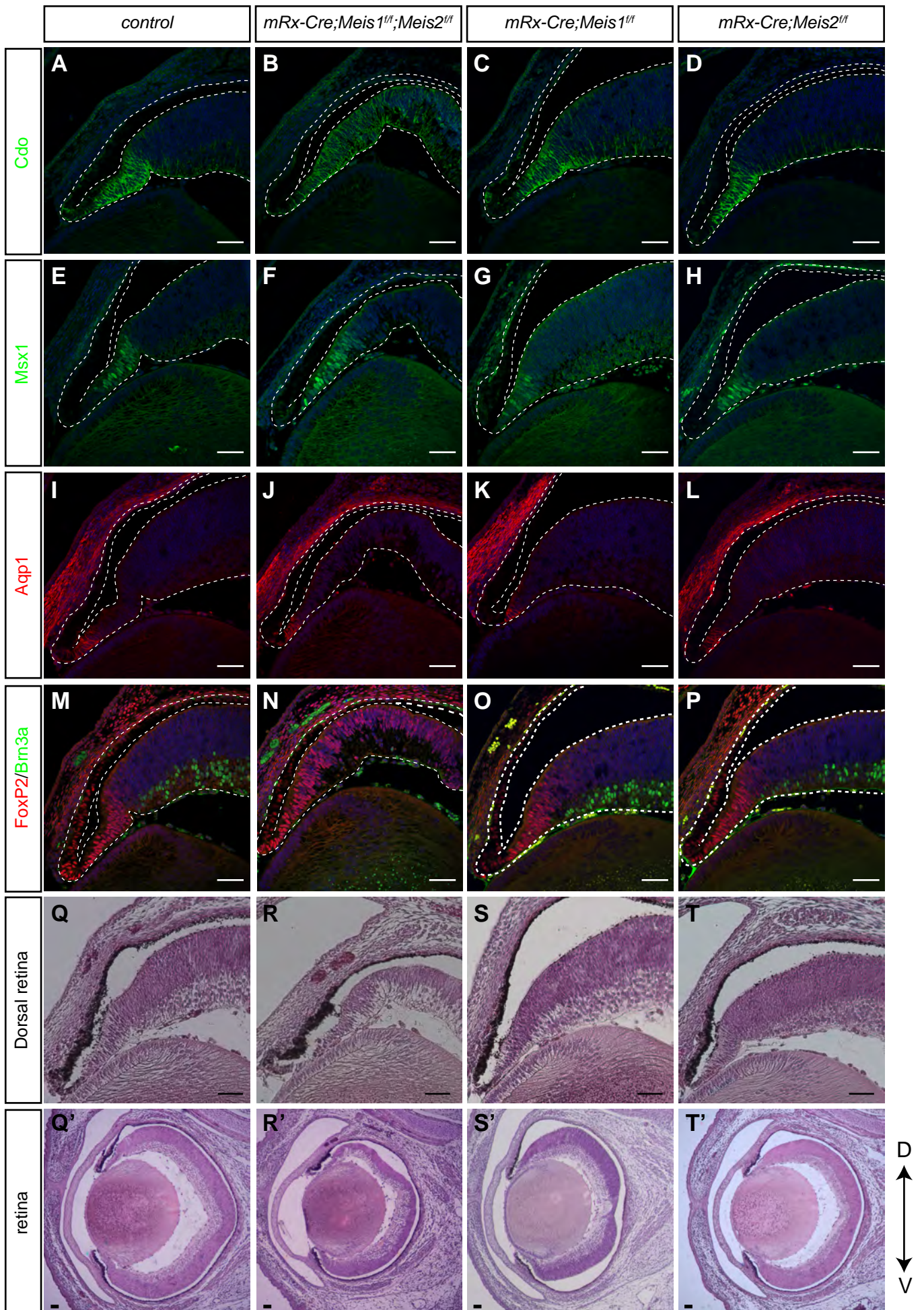
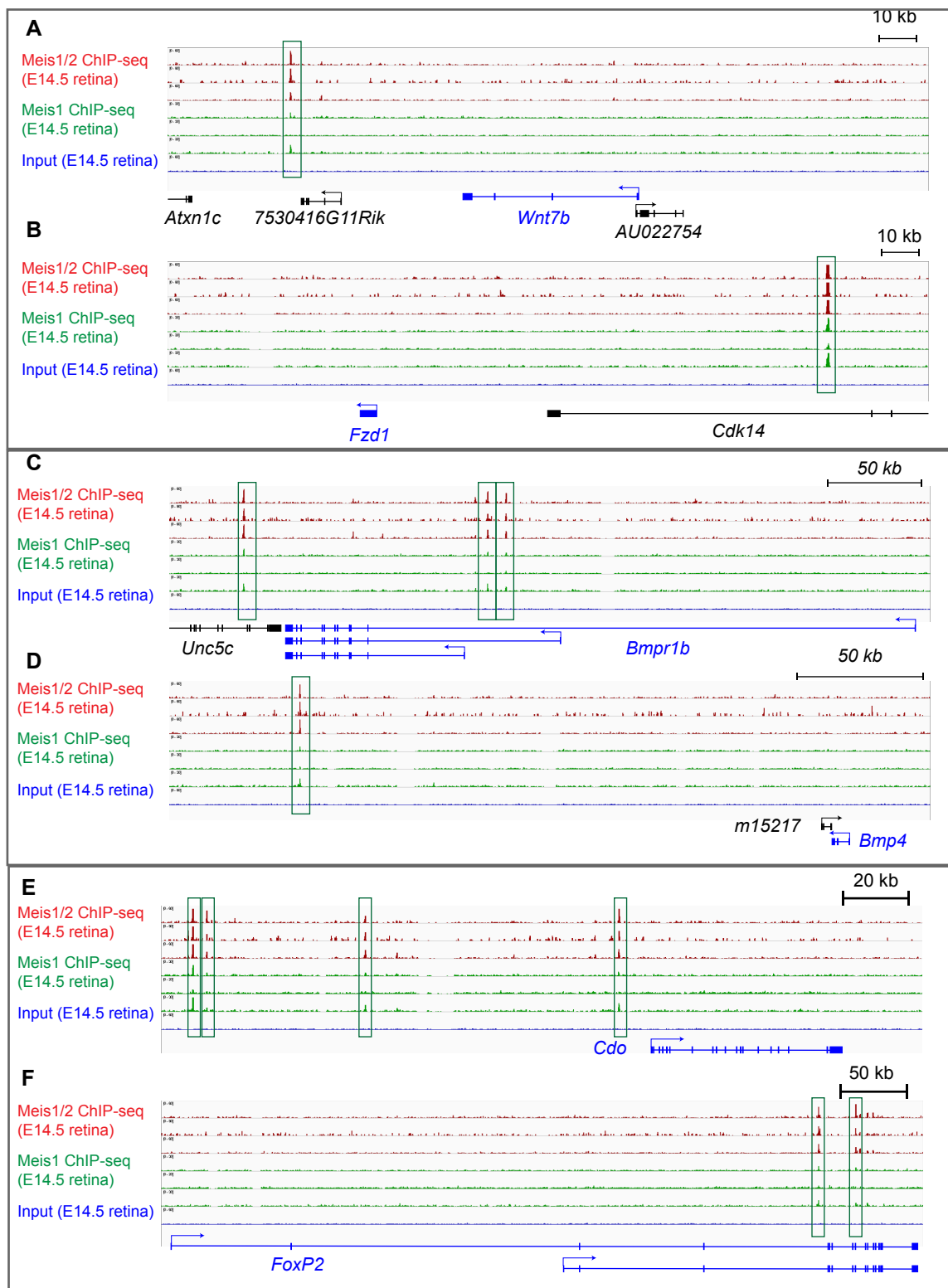


Fig. S11. CMZ is not changed in the *mRx-Cre;Meis1^{fl/fl}* and *mRx-Cre;Meis2^{fl/fl}* retinae. (A-P) Immunostaining with Cdo, Msx1, Aqp1, and FoxP2/Brn3a in frontal sections of control, *mRx-Cre;Meis1^{fl/fl};Meis2^{fl/fl}*, *mRx-Cre;Meis1^{fl/fl}* and *mRx-Cre;Meis2^{fl/fl}* embryos at E16.5. (Q-T') Haematoxylin-eosin-stained frontal sections of control and *mRx-Cre;Meis1^{fl/fl};Meis2^{fl/fl}*, *mRx-Cre;Meis1^{fl/fl}* and *mRx-Cre;Meis2^{fl/fl}* embryos at E16.5. The dorsal-ventral axis is indicated by an arrow. D: Dorsal, V: Ventral. Scale bars: 50 μ m



G

Cdo enhancer
Chr9:35369000-35369239

AGCATGCAATCTCAAAAAGGAACCCCGAGAAGCCCGAGGGCAGGGAGGGGGAGGCAGGCATGGGCAGGTTGCCAGTTCAG
CTGGTGGGAAGGCCTCCATTCTGAAAAGCATGAACATGATATTGTTTAATTTGGAGCTGACAGCTGAGAGGGAGAGGGACTGGA
TGGGGTGGGTGGGAGCCTTGACAGCCCTACTTCCAGCTCTGCAGTTTCCCATCTCCAATTGGGTTGGGAGAGGGTGGGCT

FoxP2 enhancer
Chr6:15399600-15399839

TCACTAGGCGCATGGCTACAAATTATACCTCAAGGAGGCATTCTTTGAACTTGTCACTACTGTTTCTTTTGTGATGA
CAGTGGCCATATCTTTCAAACCTAAGGCATCTCACCTAATCAGCTAAATGAATCTGACAGCTAACAATTGTTATTAAAT
CTGCTCCCTCCAGTGATAAACAAATTATACATGAAATCAATCCACTTCACAATCCTCGTCCCTATAGGGTATTATCTTTTC

Wnt7b enhancer
Chr15:85489881-85490120

AGAAGTGGGGCTGTGTAACAAGGGTCCCTGTGGGAAGATGAGCTGCTGATTATCCCGAGTTAGTTGTGGTGCCTTCACAG
ATGCATACGTGTCAAAACTTATCAAACGGTACCCCTTAATATGCACGGCTAATTTCTTGGCCATTGTACTTAAATTAAG
CTGCTTTTAAAGACAAGCAAGAGGAGCGATCCAGAAGTGAGGACCCCTTCTTGGCCAGGCTTTGCACAGCCTTGACAT

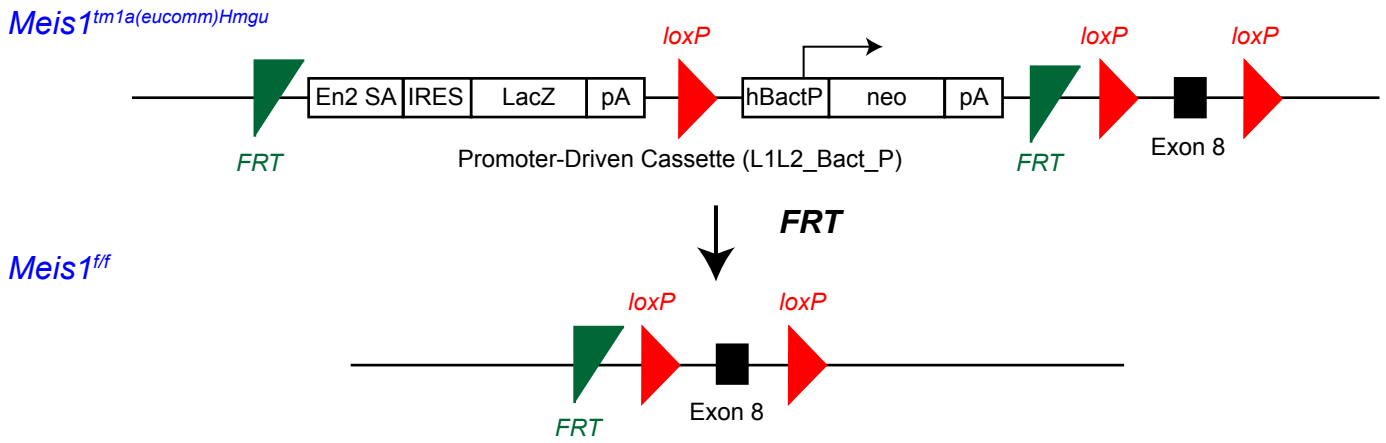
Fzd1 enhancer
Chr5:4876990-4877229

GAGTATGTCAGCTTAAATTAGTGTACATGACCCAGTCACTTTCACAGTTAAGAATAAAGAAGTTTGGCTTCTTCAAACC
CGAAGCTCAACGTGCACATTATCTAAGTTGCTTCATTACAACTCCACACTCCCTCGGGCTCATGTCAGGAGGACAGCAAT
TGTCCCTCCAGTGATAAACAAATTATACATGAAATCAATCCACTTCACAATCCTCGTCCCTATAGGGTATTATCTTTTC

Meis motif: TGACA(G/A) or (C/T) TGTC A
Sox2 motif: (A/T)TTGT, ACAA(T/A)
Homeodomain core motif (Six3): ATTA, TAAT

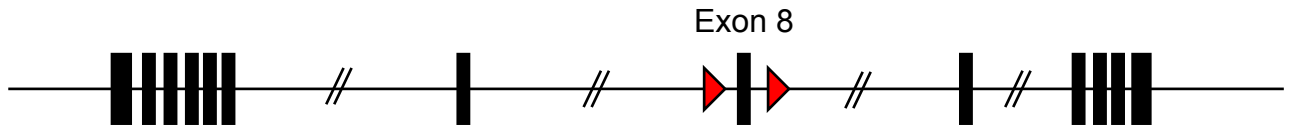
Fig. S12. Meis1 and 2 bind to the loci of Wnt/ β -catenin and BMP signalling regulator, CMZ, and optic disc-specific genes. (A-F) ChIP-seq showing Meis1/2 or Meis1 binding the loci of *Wnt7b* (A), *Fzd1* (B), *Bmpr1b* (C), *Bmp4* (D), *Cdo* (E), *Foxp2* (F). ChIP-seq peaks are indicated by green boxes. (G) The sequence of *Cdo*, *Foxp2*, *Wnt7b*, and *Fzd1* enhancers bound by Meis1/2. Meis, Sox2, and core homeodomain (Six3) motifs are indicated by red, blue, and green, respectively.

A



B

Meis1 floxed allele



Meis2 floxed allele

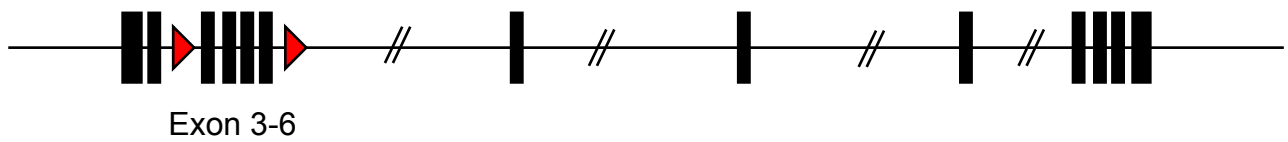


Fig. S13. Generation of *Meis1^{ff}* and *Meis2^{ff}* mice. (A) Map of the targeted *Meis1* locus before FLP-mediated removal of the FRT flanked neomycin cassette. (B) Schematic representation of targeted *Meis1* and *Meis2* loci indicating positions of inserted loxP sites.

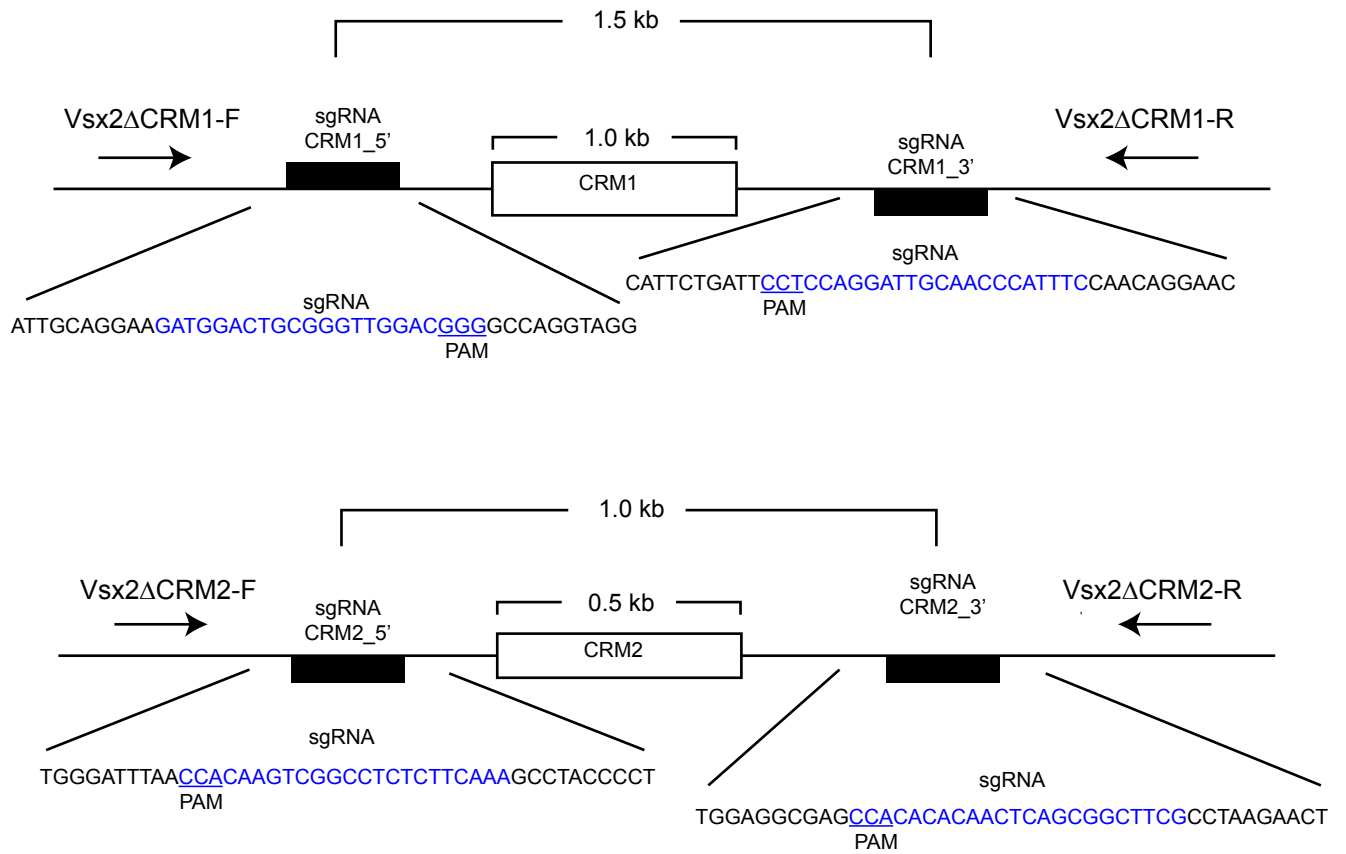


Fig. S14. Sequence map of the single guide RNAs (sgRNAs) used to generate *Vsx2 Δ CRM1*, *Vsx2 Δ CRM2*, and *Vsx2 Δ CRM1&2*. Position of primers used for confirming deletion of CRM1 and CRM2 are indicated by arrows.

Table S1. Antibodies used in this study.

Antibodies		
Rabbit polyclonal anti-Meis1 – N-terminal (1:1000)	Dr. Buchberg	N/A
Rabbit polyclonal anti-Meis2 – N-terminal (1:1000)	Dr. Buchberg	N/A
Goat polyclonal anti-Meis1/2 (ChIP-seq)	Santa Cruz	Cat# sc-10599
Rabbit polyclonal anti-Meis1 (ChIP-seq)	Abcam	Cat# ab19867
Rabbit polyclonal anti-Pax6 (1:3000)	Covance	Cat# PRB-278P
Mouse monoclonal anti-Pax6 (1:3000)	DSHB	Cat# Pax6
Goat polyclonal anti-Sox2 (1:300)	Santa Cruz	Cat# sc-17320
Sheep polyclonal anti-Vsx2 (1:500)	Chemicon	Cat# AB9014
Rat monoclonal anti-BrdU (1:500)	Abcam	Cat# ab6326
Rabbit polyclonal anti-FoxP2 (1:1000)	Abcam	Cat# ab16046
Rabbit polyclonal anti-Zic1 (1:600)	Novus	Cat# NB600-488
Goat polyclonal anti-Cdo (1:600)	R&D Systems	Cat# AF2429
Goat polyclonal anti-Msx1 (1:300)	R&D Systems	Cat# AF5045
Rabbit polyclonal anti-Aqp1 (1:300)	Millipore	Cat# 178611
Rabbit polyclonal anti-Phospho-SMAD1/SMAD5 (1:600)	Invitrogen	Cat# 700047
Rabbit polyclonal anti-Pax2 (1:300)	Invitrogen	Cat# 71-6000
Mouse monoclonal anti-Brn3a (1:300)	Millipore	Cat# MAB1585
Donkey anti-Rabbit Secondary Antibody, Alexa Fluor 594 (1:500)	Thermo Fisher Scientific	Cat# A-21207
Donkey anti-Mouse Secondary Antibody, Alexa Fluor 647 (1:500)	Thermo Fisher Scientific	Cat# A-31571
Donkey anti-Goat Secondary Antibody, Alexa Fluor 488 (1:500)	Thermo Fisher Scientific	Cat# A-11055
Donkey Anti-Sheep Secondary Antibody, Alexa Fluor 488 (1:500)	Thermo Fisher Scientific	Cat# A-11015
Donkey Anti-Mouse Secondary Antibody Alexa Fluor 488 (1:500)	Thermo Fisher Scientific	Cat# A-21202

Table S2. Primers used for genotyping.

	Primer sequence (Forward)	Primer sequence (Reverse)
<i>Meis1</i> ^{fl/fl}	ctg cgc ttc cta cat cac tg	cac ttc agc gtc act tgg aa
Vsx2 Δ CRM1	caa atc agg gca gca aaa cac	cac agg gat ggt gga aaa aca
Vsx2 CRM1 WT	ccc tgt cac ctt cat gtc tgc	cac agg gat ggt gga aaa aca
Vsx2 Δ CRM2	gcc tct gtg tcc cat gaa ctg	aaa gct ggg gac tgt cag gag
Vsx2 CRM2 WT	gcc tct gtg tcc cat gaa ctg	gga agc ccg aag ctc aca tag